Turk J Phys
33 (2009) , 209 – 217.

doi:10.3906/fiz-0812-8

Growth and microindentation analysis of pure and doped Sb_2Se_3 crystals

K. A. CHANDRASEKHARAN[1] and A. G. KUNJOMANA[2]
[1] *Dean of Science, Christ University, Bangalore, Karnataka-INDIA*
[2] *Professor, PG Department of Physics, Christ University, Bangalore, Karnataka-INDIA*
e-mail: kunjomana.ag@christuniversity.in

Received 29.12.2008

Abstract

Pure and doped antimony selenide (Sb_2Se_3, $Sb_2Se_{2.8}Te_{0.2}$, and $Sb_2Se_{2.6}Te_{0.4}$) crystals have been grown from melt by the Bridgman Stockbarger method. X-ray powder diffraction analysis was carried out to determine the lattice parameters of the grown samples. The morphology of cleavage planes was observed using SEM. Energy dispersive analysis by X-rays (EDAX) was done to find out the chemical composition of the grown samples. Correlation of microhardness with other mechanical characteristics such as toughness, brittleness, and yield strength, has been investigated. The effects of Te doping on the mechanical behaviour and energy gap were also studied on the cleavage faces.

Key Words: Sb_2Se_3, microindentation, energy gap, doping.
PACS: 81.10.-h, 81.10.Fq, 62.20.-x

1. Introduction

The V-VI group compounds are useful semiconductors and find application in television cameras with photoconducting targets, thermoelectric devices, electronic and optoelectronic devices, and infrared spectroscopy [1, 2]. Antimony selenide (Sb_2Se_3) belongs to V-VI group semiconductors, and exhibits good photovoltaic properties and high thermoelectric power, which allow possible applications for optical and thermoelectronic cooling devices [3]. It has also received a great deal of attention due to its switching effects [4, 5]. Hence, the synthesis and characterization of these compounds have been investigated by many researchers [6-12].

Sb_2Se_3 is a direct band gap semiconductor with an energy gap of 1.2 eV [12, 13]. It crystallizes in orthorhombic phase with cell dimensions $a = 11.62 \pm 0.01$ Å, $b = 11.77 \pm 0.01$ Å and $c = 3.962 \pm 0.007$ Å [14]. The melting point of antimony selenide is 611 °C and density is 5810 kg/m^3. Various methods have been employed for the growth of antimony selenide crystals. Bacewicz and Ciszek [9] have reported

liquid encapsulated crystal growth and electrical properties of Sb_2Se_3. The growth of crystalline Sb_2Se_3 whiskers has been conducted via a hydrothermal process by Wang et al. [15]. Arivuoli et al. [2] have grown Sb_2Se_3 platelet and needle crystals from vapour in a two-zone furnace. Several authors have investigated the microindentation analysis of pure and doped semiconducting crystals. Nagabhooshanam and Haribabu [16] have reported the Vickers microhardness studies on III-V and II-VI compound semiconducting crystals. The microhardness measurements of Si, GaP, GaAs and InP single crystals were carried out by Feltham and Banerjee [17]. Jani et al. [18] have studied the effect of impurity on the hardness and deformation properties of InBi single crystals. Kunjomana and Chandrasekharan [19] have given an account on the dislocation and microindentation analysis of $Bi_2Te_{3-x}Se_x$ whiskers. The study of Vickers microhardness on $InBi_{0.85}Sb_{0.15}$ single crystals was reported by Shah et al. [20].

Although the electrophysical properties of Sb_2Se_3 crystals have been studied to quite a good extent, very little information is available in the literature on the study of mechanical properties of melt grown antimony selenide single crystals. To the best of our knowledge, the influence of Te doping on mechanical characteristics such as hardness, toughness and brittleness of Sb_2Se_3 crystals has not been reported so far. As such, the present authors have grown Sb_2Se_3, $Sb_2Se_{2.8}Te_{0.2}$, and $Sb_2Se_{2.6}Te_{0.4}$ single crystals by melt growth method and have studied the load dependence of microhardness on the cleavage planes of these crystals. Attempts have been made to determine the toughness of cleaved samples by measuring the crack length and thus the brittleness was evaluated. The values of yield strength and energy gap of pure and doped crystals were determined. The results on correlation of mechanical properties were explained in terms of the change in chemical composition on deformation-induced regions of cleavage faces. The Meyer index otherwise known as the work-hardening exponent has been computed using least squares fit analysis and the results were discussed.

2. Experimental

Sb_2Se_3, $Sb_2Se_{2.8}Te_{0.2}$ and $Sb_2Se_{2.6}Te_{0.4}$ crystals were grown by the Bridgman Stockbarger method. Appropriate quantities of the constituent elements of 99.99% purity were vacuum sealed in pre-cleaned quartz ampoule of length 10 cm and diameter 10 mm under pressure of 10^{-5} torr. The sealed ampoule was kept in a constant temperature muffle furnace at 700 °C for about 24 h, during which the ampoule was periodically rotated for proper mixing and reaction of the constituents. The ingots were then slowly cooled to room temperature. The growth was carried out in a vertical gradient furnace by keeping the ampoule at 650 °C for 48 h and then lowered at a rate of 0.5 mm per minute. The crystals grown were cleaved at ice temperature to minimize deformation. The morphology of cleaved samples was observed using a scanning electron microscope (Jeol JSM-840 A). X-ray diffraction studies of Sb_2Se_3 crystals were carried out with Ni filtered CuKα radiation (λ=1.54060 Å) using a Philips X'pert diffractometer. The chemical analysis was also done using EDAX to determine the composition of the crystals.

The microhardness measurements were carried out on the cleaved planes at room temperature using a Vickers diamond pyramidal indenter [19]. The indentations were made at different loads from 2.5 to 40 g, above which intensive cracking was observed. The indentation time was kept at 15 sec for all the samples. Hardness H_V was computed using the relation

$$H_V = 1.8544p/d^2 \tag{1}$$

where p is the load in kg and d is the mean diagonal length in mm. The toughness, defined as the resistance to fracture of a material was calculated according to the expression

$$K_c = \frac{p}{\beta_o l^{3/2}}, \tag{2}$$

where β_o is the indenter constant and l is the crack length in μm.

The brittleness index B_i, which implies the relative susceptibility of a material to two competing mechanical responses, deformation and fracture, is an important property as far as the mechanical behaviour of a material is concerned. According to Lawn and Marshall [21], the ratio H_v / K_c gives the value of brittleness. The yield strength Y of the samples is determined using the relation $Y = H_v/3$. The energy gap of semiconducting compounds is correlated to microhardness H_v using the formula [22]

$$E_g = \frac{H_v V_{cell}}{1.6 \times 10^{-19} \times 10^2}. \tag{3}$$

Here, E_g is the gap height in eV, H_v has units of kg/mm^2, and the unit cell volume V_{cell} has units of mm^3.

3. Results and discussion

Single crystals of antimony selenide having 30 mm long and 10 mm in diameter were obtained, as shown in Figure 1. Figure 2 shows the SEM image of a freshly cleaved surface of the antimony selenide crystal. In Figure 3, the powder XRD patterns of pure and doped Sb_2Se_3 crystals are depicted. The X-ray diffractograms with peak characteristics revealed the crystallinity of the grown samples. The diffraction peaks in the pattern are indexed to the orthorhombic phase.

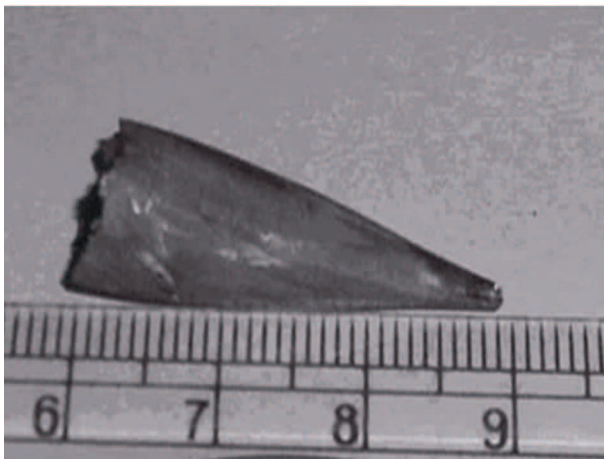

Figure 1. Sb_2Se_3 crystal grown by Bridgman Stockbarger method.

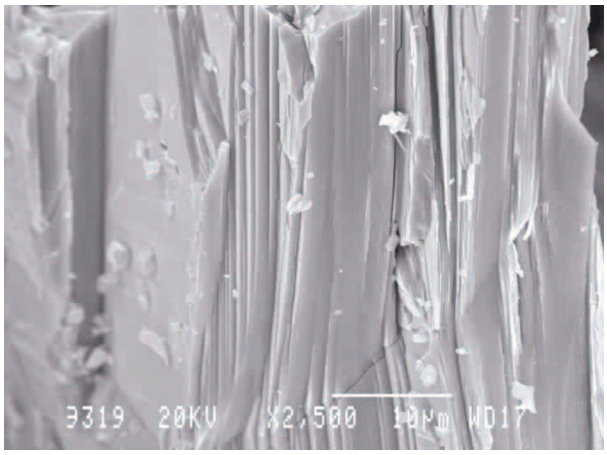

Figure 2. SEM image of a cleaved surface showing parallel steps.

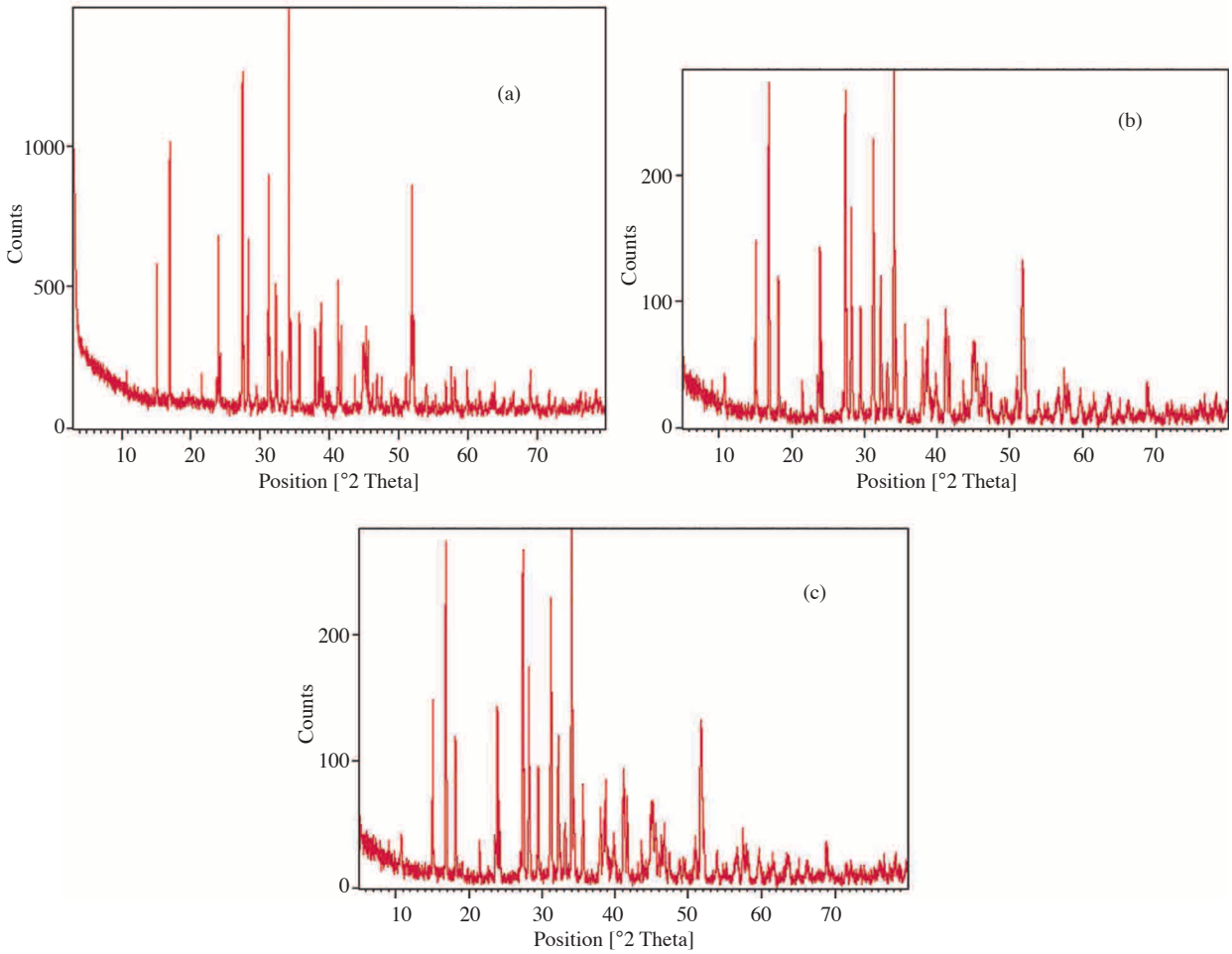

Figure 3. Powder X-ray diffractograms of antimony selenide crystals: (a) Sb_2Se_3 (b) $Sb_2Se_{2.8}Te_{0.2}$, and (c) $Sb_2Se_{2.6}Te_{0.4}$ samples.

The Table below shows the calculated values of lattice constants and cell volume, from the XRD data, which are fairly in agreement with the values reported by Tideswell et al. [14]. The values of cell parameters are found to be increased for Te doped samples.

Table. Crystallographic data and energy gap of antimony selenide single crystals.

Sample	a (Å)	b (Å)	c (Å)	V(Å^3)	Eg (eV)
Sb_2Se_3	11.62	11.76	3.958	540.865	1.219
$Sb_2Se_{2.8}Te_{0.2}$	11.63	11.77	3.968	543.160	1.211
$Sb_2Se_{2.6}Te_{0.4}$	11.66	11.78	3.969	545.161	1.205

The compositional analysis of Sb_2Se_3, $Sb_2Se_{2.8}Te_{0.2}$, and $Sb_2Se_{2.6}Te_{0.4}$ crystals are represented in Figure 4. The EDAX analysis showed the presence of constituent elements in the grown samples. The proportion of Te contents in Sb_2Se_3, $Sb_2Se_{2.8}Te_{0.2}$, and $Sb_2Se_{2.6}Te_{0.4}$ samples are found to be in the ratio 0:7.22:15.16 at%.

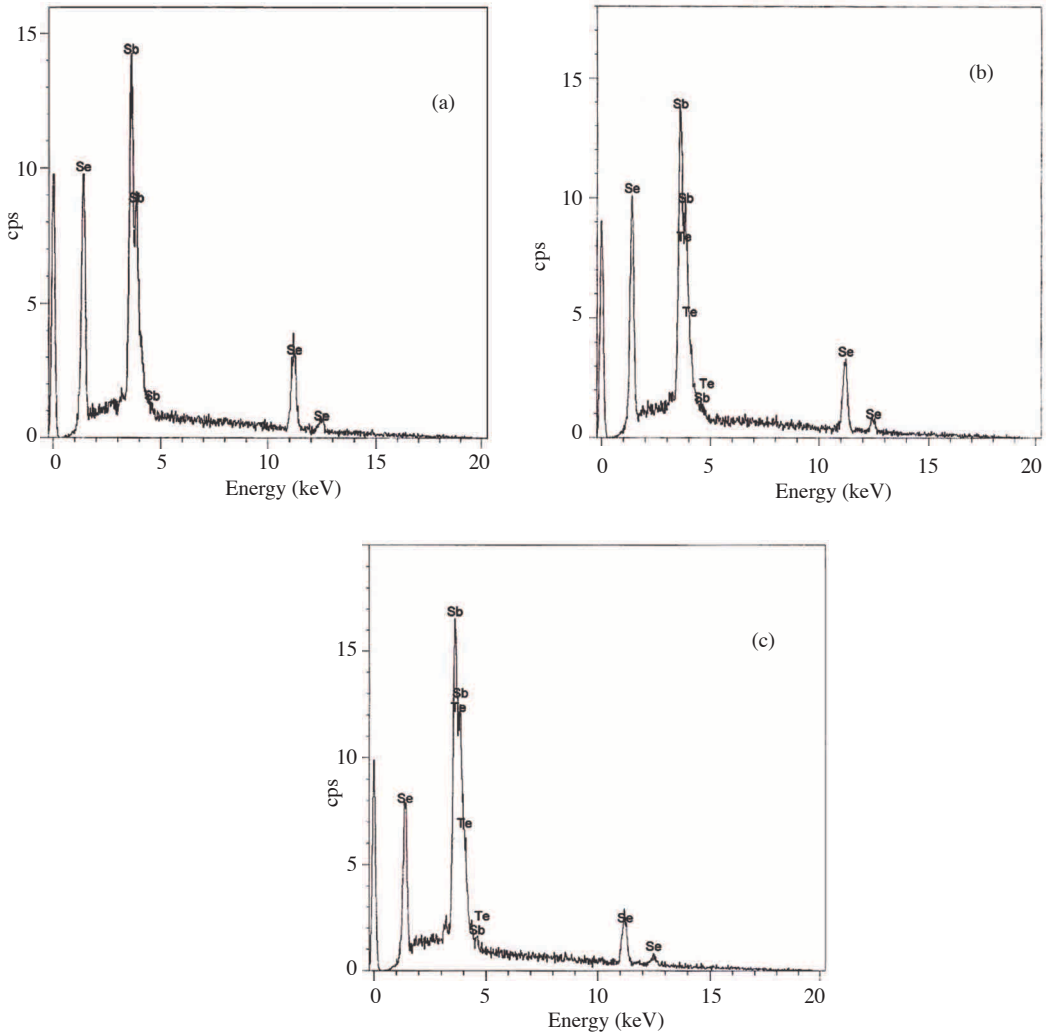

Figure 4. EDAX profiles of (a) Sb_2Se_3, (b) $Sb_2Se_{2.8}Te_{0.2}$, and (c) $Sb_2Se_{2.6}Te_{0.4}$ crystals.

Sb_2Se_3 is a layer structured compound, whose structure consists of chain like arrangement of Sb and Se atoms parallel to the c-axis [14]. Pairs of these chains are fastened together along 2_1 screw axis to form larger chains through sets of Sb-Se bonds of length 0.298 nm. These larger chains are, in turn, bonded into sheets roughly perpendicular to the b-axis through sets of Sb-Se bonds, which are 0.326 nm in length. Finally, the sheets are held together to make the crystalline solid through two sets of Sb-Se bonds, which are respectively 0.346 and 0.374 nm long. It is possible to think of this structure as made up of puckered sheets or planes of stoichiometric composition running parallel to the c-axis, and more or less in the (010) direction. The binding between these sheets is considerably weaker than that within the sheets. This suggests that cleavage takes place more or less on (010) planes by breaking the two sets of Sb-Se bonds of length 0.346 and 0.374 nm. The most striking feature of layered type crystals is the existence of easy cleavage and since the cleavage planes are easy to glide, some deformation may accompany the cleavage step foromation process. The deformation characteristics affect the mechanical behaviour of the samples. Since the cleavage surfaces are never atomically smooth, it is important to understand their irregularities. In reality, they present a system of steps very nearly parallel to

the cleavage direction, as shown in Figure 2. The grown crystals with smooth cleaved surfaces and free from any microstructures are selected for the indentation studies.

Hardness testing provides useful information concerning the mechanical characteristics of materials such as toughness, brittleness, yield strength, etc. The variation of hardness with load on the cleavage surfaces of pure and doped antimony selenide crystals is shown in Figure 5. The decrease in hardness of antimony selenide crystals with increase in load is due to their greater tendency towards crack formation and plastic deformation. Since the cleavage plane is easy to glide, it will slip during the indentation process. Hence as the load is increased, the amount of plastic strain is also increased, which in turn reduces the microhardness value. The hardness attains a constant value ($\sim$35 kg/mm^2), beyond a load of 20 (g) due to decrease in the resistance to the movement of dislocations. The intrinsic strength of chemical bonds on the cleavage planes also plays a prime role in determining the hardness of semiconducting compounds [19].

A plot of the square of the length of diagonal, d^2 (mm^2) against load p (g) gave a straight line passing through the origin as shown in Figure 6, indicating that there is no loading error in the studied range of loadings [23]. According to Meyer's law, $p = ad^n$, where p is the load applied (g), d is the diagonal length (mm), n is the Meyer index and a is a constant for a given material. Figure 7 shows the graph of log d versus log p drawn using the hardness data of Sb_2Se_3 crystals. Similar observations were found for $Sb_2Se_{2.8}Te_{0.2}$, and $Sb_2Se_{2.6}Te_{0.4}$ crystals.

The values of n determined using least squares fit method for Sb_2Se_3, $Sb_2Se_{2.8}Te_{0.2}$, and $Sb_2Se_{2.6}Te_{0.4}$ crystals were found to be 1.9333, 1.9230, and 1.9285 respectively. This result supports the concept of Onitsch [24] that if $n < 2$, the hardness decreases with increasing load. The computed values of energy gap, E_g = 1.219 eV for Sb_2Se_3 is in agreement with that reported earlier [12, 13], which indicated the consistent results of hardness and cell volume. The energy gap values are found to decrease with Te doping. The average value of yield strength for Sb_2Se_3, $Sb_2Se_{2.8}Te_{0.2}$, and $Sb_2Se_{2.6}Te_{0.4}$ crystals is found to be 0.1179 GPa, 0.1166 GPa, and 0.1156 GPa, respectively.

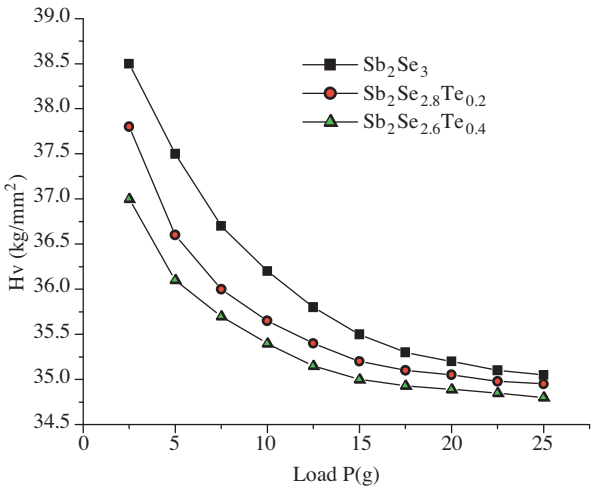

Figure 5. Variation of microhardness with applied load.

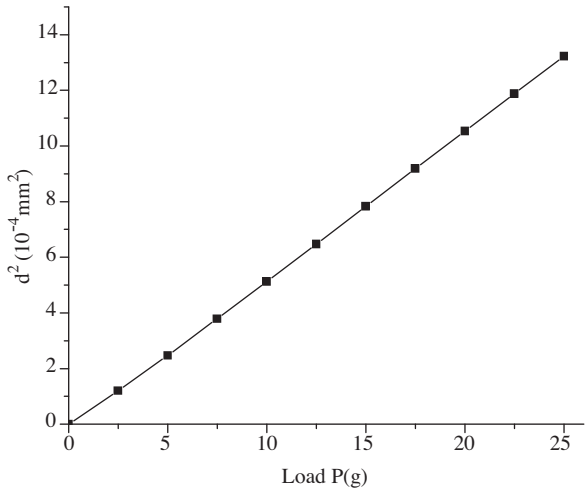

Figure 6. Variation of d^2 with applied load p of Sb_2Se_3 crystals.

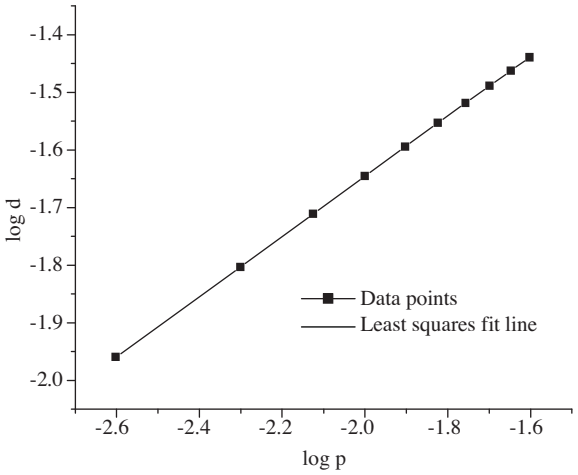

Figure 7. Meyer plot between log d and log p of Sb_2Se_3 crystals.

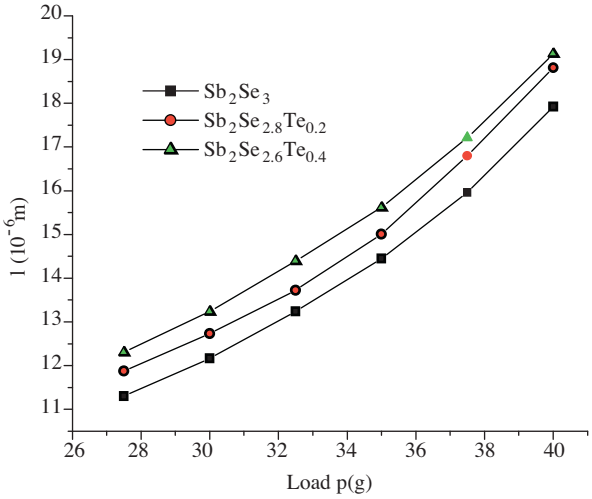

Figure 8. Plot of crack length versus load.

Fracture toughness, K_c, is an important material parameter in the application of brittle solids. Among the experimental methods available for the measurement of toughness [25–27], the indentation method is the best suited for materials with low toughness value. As load was increased, cracks were initiated in all samples and the crack length increased with load (Figure 8). During indentations, radial cracks have been observed on the cleavage faces at higher loads. Several median vents growing simultaneously from the stress concentration points, due to the sharp indenter edges, were also found.

Lawn and Wilshaw [28, 29] have discussed the basic sequence of crack propagation events. The sharp points of indenter produces an inelastic deformation and, at some threshold, induces a deformation-induced flow that suddenly develops into crack, with the median vent on a plane containing the contact axis, and the increase in load causes further stable growth of the median vent. On unloading, the median vents begin to close, but not heal. The applied load further develops, extending cracks called lateral vents, which continue to extend and cause chipping.

For loads greater than 25 g, the cracks were large compared with the impression diagonal. In the present study, loads beyond 40 g were not used for the evaluation of toughness as chipping of material occurs above this load. The toughness value was found to decrease with increase in load as shown in Figure 9. It is seen from Figures 5 and 9 that, hardness and toughness values are decreased for $Sb_2Se_{2.8}Te_{0.2}$, and $Sb_2Se_{2.6}Te_{0.4}$ samples. This is because, when selenium of ionic radius 0.69 **Å** is replaced by tellurium of larger ionic radius 0.81 Å, generation of vacancies is comparatively lesser in $Sb_2Se_{2.8}Te_{0.2}$, and $Sb_2Se_{2.6}Te_{0.4}$ crystals than in Sb_2Se_3 crystals. Hence they do not act as barriers to dislocation movement [19], causing a decrease in resistance to deformation and fracture. Thus the tellurium doping decreases the values of hardness and toughness. The brittleness index is governed by both hardness and fracture toughness together on the deformation induced cleavage faces. As the composition of tellurium increases, the brittleness increased due to the development of cracks during indentation process as shown in Figure 10.

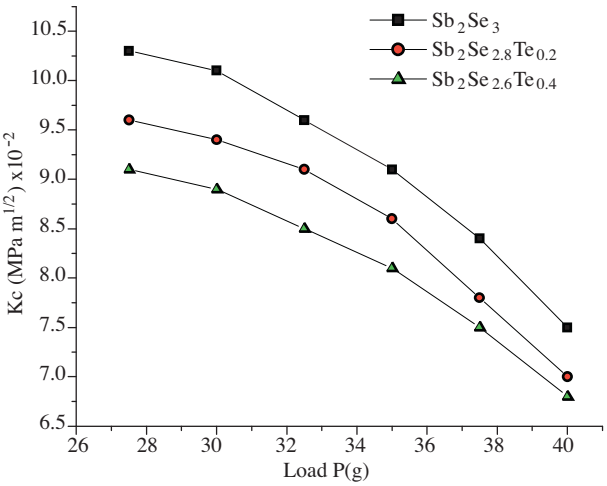

Figure 9. Variation of toughness with load.

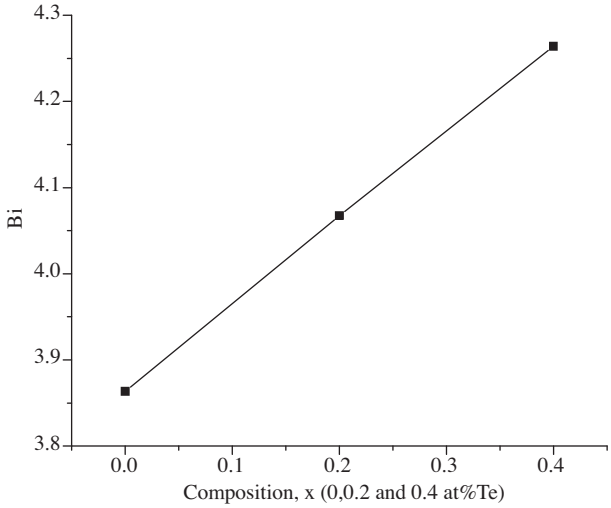

Figure 10. Brittleness as a function of increase in Te content of Sb_2Se_3 crystals.

4. Conclusion

Single crystals of Sb_2Se_3, $Sb_2Se_{2.8}Te_{0.2}$, and $Sb_2Se_{2.6}Te_{0.4}$ were grown by the Bridgman Stockbarger method. X-ray diffraction studies revealed that, the grown crystals have orthorhombic structure. The calculated parameters agreed with that reported in the literature. The lattice constants and cell volume are found to increase for Te doped samples. The microhardness was found to decrease with applied load and then become constant for all samples. The EDAX spectra showed the change in chemical composition of samples with increase in Te and confirmed the presence of constituent elements. On doping with Te, hardness and toughness values were decreased and brittleness increased. The energy gap of Sb_2Se_3 crystals is found to be 1.219 eV, whereas it slightly reduces for $Sb_2Se_{2.8}Te_{0.2}$ and $Sb_2Se_{2.6}Te_{0.4}$ crystals.

Acknowledgements

The authors would like to thank the U.G.C., New Delhi for financial support. Thanks are due to Prof. K. L. Sebastian, Chairman, Department of Inorganic and Physical Chemistry, I.I.Sc, Bangalore for providing facilities to do vacuum sealing of ampoules. The help rendered by the research group in Department of Physics and Department of Metallurgy, I.I.Sc, Bangalore is also gratefully acknowledged in connection with XRD, SEM and EDAX analysis. Thanks to Mr. V. Sivanandam of I.I.T Madras and Prof. E. Mathai for their research assistance.

References

[1] W. Wang, B. Poudel, J. Yang, D. Z. Wang and J. F. Ren, *J. Am. Chem. Soc.*, **127,** (2005), 13792.

[2] D. Arivuoli, F. D. Gnanam and P. Ramasamy, *J. Mater. Sci. Lett.*, **7**, (1988), 711.

[3] K. Y. Rajpure, C. D. Lokhande and C. H. Bhosale, *Mater. Res. Bull.*, **34**, (1999), 1079.

[4] N. Platakis and H. Gatos, *Phys. Status Solidi* A, **13**, (1972), K1.

[5] I. Kim, *Mater. Lett.*, **43**, (2000), 221.

[6] A. A. Babaev, *J. Appl. Spectroscopy*, **22**, (1975), 44.

[7] J. Shen and R. Blachnik, *Thermochimica Acta,* **399**, (2003), 245.

[8] C. Zhao, X. Cao and X. Lan, *Mater. Lett.*, **61**, (2007), 5083.

[9] R. Bacewicz and T. F. Ciszek, *J. Cryst. Growth*, **109**, (1991), 313.

[10] B. R. Chakraborty, B. Roy, R. Bhattacharya and A. K. Dutta, *J. Phys. Chem. Solids*, **41**, (1980), 913.

[11] F. Kosek, J. Tulka and L. Stourac, *Czech. J. Phys.*, **28**, (1970), 325.

[12] M. Kurumada, H. Suzuki, Y. Kimura, Y. Saito and C. Kaito, *J. Cryst. Growth*, **250**, (2003), 444.

[13] L. R. Gilbert, B. van Pelt and C. Wood, J. *Phys. Chem. Solids*, **35**, (1974), 1629.

[14] N. W. Tideswell, F. H. Kruse and J. D. McCullough, *Acta Cryst.*, **10**, (1957), 99.

[15] D. Wang, Yu Dabin, M. Shao, J. Xing and Y. Qian, *Mater. Chem. Phys.*, **82**, (2003), 546.

[16] M. Nagabhooshanam and V. Haribabu, *Cryst. Res. Technol.*, **20**, (2006), 1399.

[17] P. Feltham and R. Banerjee, *J. Mater. Sci.*, **27**, (1992), 1626.

[18] T. M. Jani, G. R. Pandya and C. F. Desai, *Cryst. Res. Technol.,* **29**, (1994), K3.

[19] A. G. Kunjomana and K. A. Chandrasekharan, *Cryst. Res. Technol.*, **43**, (2008), 594.

[20] D. Shah, G. R. Pandya, S. M. Vyas and M. P. Jani, *Turk. J. Phys.*, **31**, (2007), 231.

[21] B. R. Lawn and D. B. Marshall, J. *Amer. Ceram. Soc.*, **62**, (1979), 347.

[22] J. J. Gilman, *The Science of hardness testing and its research application, eds.* J. H. Westbrook and H. Conrad, (American Society for Metals, Ohio, 1971), p. 51.

[23] C. C. Desai and J. L. Rai, *Bull. Mater. Sci.*, **5**, (1983), 453.

[24] E. M. Onitsch, *Mikroskopie,* **2**, (1947), 131

[25] A. G. Evans and E. A. Charls, *J. Amer. Ceram. Soc.,* **59**, (1976), 371.

[26] B. R. Lawn and E. R. Fuller, *J. Mater. Sci.,* **10**, (1975), 2016.

[27] J. J Petrovic, L. A. Jacobson, P. K. Talty and A. K. Vasudevan, *J. Amer. Ceram. Soc.*, **58**, (1975), 113.

[28] B. Lawn and R. Wilshaw, *J. Mater. Sci.,* **10**, (1975), 1049.

[29] B. Lawn and R. Wilshaw, *J. Non - Cryst. Solids,* **38**, (1980), 391.